Canadian Mineralogist
Vol. 20, pp. 239-251 (1982)

THE CRYSTAL STRUCTURE OF A CARBONATE-RICH CANCRINITE

H. D. GRUNDY AND I. HASSAN
Department of Geology, McMaster University, Hamilton, Ontario L8S 4L8

ABSTRACT

The crystal structure of a carbonate-rich cancrinite has been refined to a conventional R index of 2.8% in space group $P6_3$ using X-ray-diffraction data and a model derived using a study by high-resolution transmission electron microscopy and detailed Fourier sections from a trial refinement. The superstructure observed can be rationalized solely in terms of the substitutional arrangement of interchannel cations and anions on sites positionally consistent with the space-group symmetry. Stacking variations differing from the hexagonal ABAB... type are shown not to exist in this material.

Keywords: cancrinite, X-ray diffraction, crystal structure, high-resolution transmission electron microscopy, superstructure, sodalite, zeolite.

SOMMAIRE

La structure cristalline d'une cancrinite riche en carbonate a été affinée dans le groupe spatial $P6_3$ jusqu'à un résidu R de 2.8%. L'affinement est fondé sur données de diffraction X et à la lumière d'une étude au microscope électronique par transmission à haute résolution et de sections de Fourier détaillées résultant d'un affinement préliminaire. On explique la surstructure observée en fonction de l'agencement des substitutions des cations et anions dans les positions permises par le groupe spatial. On montre qu'aucune déviation de la séquence d'empilement hexagonal ABAB... n'existe dans ce matériau.

(Traduit par la Rédaction)

Mots-clés: cancrinite, structure cristalline, diffraction X, microscopie électronique par transmission à haute résolution, surstructure, sodalite, zéolite.

INTRODUCTION

The cancrinite group of minerals is characterized by an ordered framework of (Al, Si) O_4 tetrahedra. The hexagonal symmetry is the result of the close packing of interconnected and parallel 6-fold rings of alternating AlO_4 and SiO_4 tetrahedra in an ABAB... type of stacking sequence (Jarchow 1965). Many members of the sodalite group of minerals are polymorphic with members of the cancrinite group. However, the latter have cubic symmetry due to an ABCABC... stacking sequence. The difference in stacking sequence gives rise to important structural dissimilarities between the two mineral groups.

Cancrinite has a large continuous framework channel parallel to the axis of 6-fold rotation (z axis), in which are located interframework cations and anions. In sodalite this channel is offset by the C-type stacking layer to give a network of large cages. In addition, cancrinite has "chains" of small cages parallel to the z axis. These consist of framework cavities between successive A- or B-type layers (Fig. 1); these cavities also contain cations and anions. The difference in structure between these two groups suggests that the cancrinite-group minerals are more likely to be the low-temperature polymorphs, as the continuous channel facilitates diffusion, and thereby decomposition, at elevated temperatures. In the case of the hydroxy varieties, this has been experimentally verified (van Peteghem & Burley 1962).

Although the frameworks of these groups of minerals are well defined and essentially a 1:1 ratio of AlO_4 and SiO_4 tetrahedra, the interframework ions are chemically diverse and typical of zeolitic materials. The large channels in cancrinite are found to contain Na^+, K^+, Ca^{2+}, OH^-, CO_3^{2-}, SO_4^{2-} or H_2O and the small cages, Na^+, K^+, Ca^{2+}, OH^-, H_2O or Cl^-; the sodalite-group cavity can contain Na^+, K^+, Ca^{2+}, OH^-, SO_4^{2-}, Cl^- or H_2O. The disorder that results from substitution of these ionic species for each other gives $P6_3$ symmetry. As a further complication, vacancies on non-framework sites are usual in both groups of minerals.

The general features of the crystal structures of both cancrinite and sodalite are well known (Pauling 1930). However, the detailed structure and the origin of observed superstructures are not clear. This work reports on some of the results of a general study of the structure and chemistry of these two groups of minerals.

EXPERIMENTAL

Although useful models of the crystal struc-

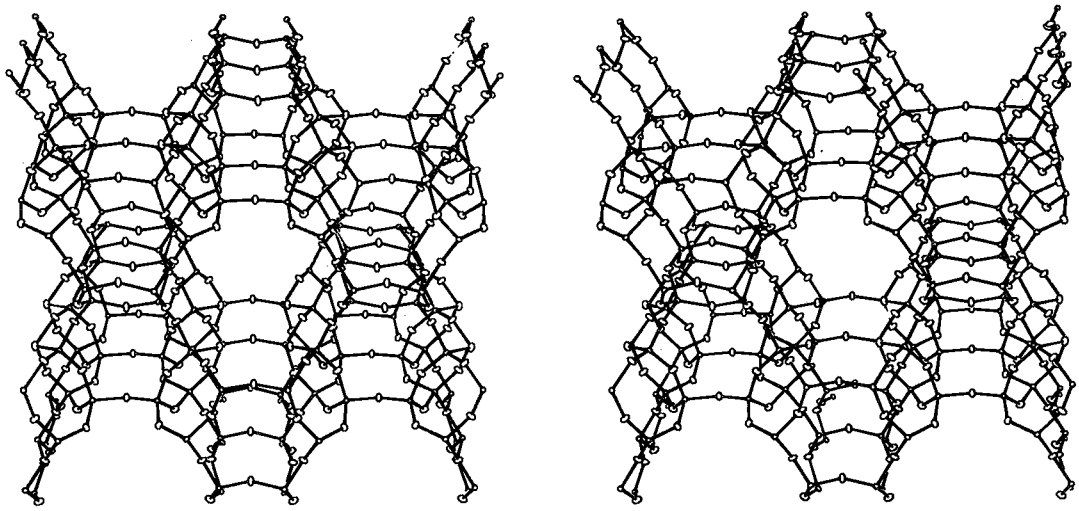

FIG. 1. Stereographic schematic diagram of the framework of cancrinite viewed down the z axis. The large channel is defined by the "chains" of interconnected small cages parallel to the z axis.

ture of the sodalite-group minerals have been established (Schulz 1970), those for the cancrinite group are less detailed (Jarchow 1965, Nithollon & Vernotte 1955). Therefore, in the initial stages of the present research program, a structural refinement of a possible "end-member" cancrinite was undertaken to define a model that would be a useful starting point for the refinement of chemically more complex species. Details of the material chosen are given in Table 1.

Long-exposure precession photographs (Fig. 2) show a symmetry consistent with the accepted space-group $P6_3$ (Jarchow 1965). The diffraction photographs also show a well-developed superstructure resulting in a supercell consistent with a c dimension eight times that of the substructure. All observed diffraction maxima are sharp. Cell dimensions, determined by least squares from 25 substructure reflections automatically aligned on a 4-circle diffractometer, are presented in Table 1 together with other information pertaining to the collection and refinement of X-ray data. A sphere 0.2 mm in diameter was ground and used to collect the intensity data. The crystal was mounted on a Syntex $P2_1$ automatic diffractometer using graphite-monochromated Mo$K\alpha$ radiation and operated in the θ–2θ scan mode. A total of 1918 reflections were collected over two asymmetric units out to a 2θ value of 65°. During the data acquisition, standard reflections collected at regular intervals indicated that there was deterioration neither in crystal quality nor crystallographic alignment. The data were corrected for spherical absorption, Lorentz, polarization and background effects and subsequently reduced to structure factors. All crystallographic

TABLE 1. CRYSTAL DATA FOR CANCRINITE FROM BANCROFT, ONTARIO†

Chemical analysis††		Cell Contents†††		Miscellaneous
SiO_2	34.35	Si	5.98	a 12.590(3) Å
Al_2O_3	29.35	Al	6.02	c 5.117(1) Å
Fe_2O_3	.03	Fe	.03	V 702.4(3) Å^3
MgO	.01	Mg	.03	Space Group $P6_3$
				Z 1
CaO	8.11	Ca	1.52	Density Calc. 2.37 gm/cc
				μ 10.28 cm^{-1}
Na_2O	17.66	Na	5.96	Crystal Size sphere 0.2 mm diameter
K_2O	.10	K	.02	Rad MoK_α graphite monochromator
H_2O^+	3.02	H_2O	1.75	Total no. of I 1918
H_2O^-	.11			Non equiv. 942
				$\|Fo\| > 3\sigma$ 855
CO_2	6.60	C	1.57	Final R(obs) = 2.8
				$= \sum(\|F_o\|-\|F_c\|)/\sum\|F_o\|$
Cl	.21	Cl	.06	Final R_w(obs) = 3.1
				$= (\sum w(\|F_o\|-\|F_c\|)^2/$
				$\sum w\|F_o\|^2)^{1/2}$
S	n.d.			w = 1
wt %	99.55			

Chemical formulae used in refinement
$Na_6\ Si_6\ Al_6\ O_{24}\ Ca_{1.5}\ 1.6CO_3$

† specimen 68024, McMaster University collection. From Dungannon Township, Ontario.
†† wet analysis, J. Muysson, McMaster University (H_2O^+ by Penfield gravimetric method).
††† based on Al + Si = 12

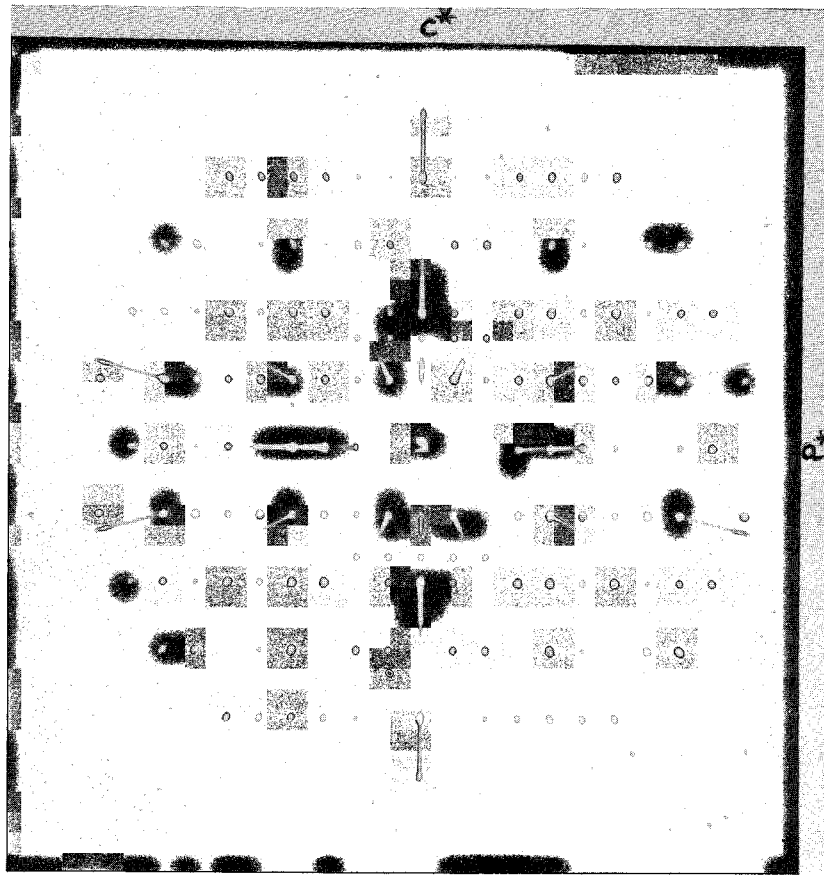

FIG. 2. Zero-level [100]-axis X-ray-diffraction photograph of cancrinite, showing strong substructure reflections with generally much weaker superstructure reflections in rows parallel to a^* ($\mu = 30°$, Cu$K\alpha$ radiation, Ni filter).

calculations were made using the X-RAY76 Crystallographic System (Stewart *et al.* 1976).

A reflection was considered observed if its magnitude exceeded that of three standard deviations based on counting statistics. This resulted in 942 unique reflections of which 855 were classified as observed. A trial refinement of the crystal structure was made by the least-squares method using the structure previously determined by Nithollon & Vernotte (1955) as the starting model. Scattering factors for neutral atoms were taken from Doyle & Turner (1968). The refinement converged at a conventional R-index of $\sim$ 7% after varying the scale, positional parameters and anisotropic temperature-parameters. The refinement was constrained according to the chemical formula (Table 1). The refined structure showed satisfactory geometry for the framework. The lengths of both the Si–O and Al–O bonds were compatible with ordered alternating AlO_4 and SiO_4 tetrahedra, and the temperature factors for both Al, Si and the framework oxygen atoms showed nothing unusual. The large channel cation was positionally well defined and had normal temperature-factors, in marked contrast to the anion group (CO_3^{2-}) position, which showed an extremely anisotropic thermal vibration with elongation parallel to the z axis. The small-cage cation, which lies on a special position on the 3-fold axis, also showed large anisotropy parallel to the z axis, whereas the oxygen in this cage showed a disc-shaped thermal ellipsoid elongate perpendicular to the z axis. These observations are in accord with those made by Jarchow (1965) from a structure refinement of similar material. A projection of this trial structure down [001] is shown in Figure 3.

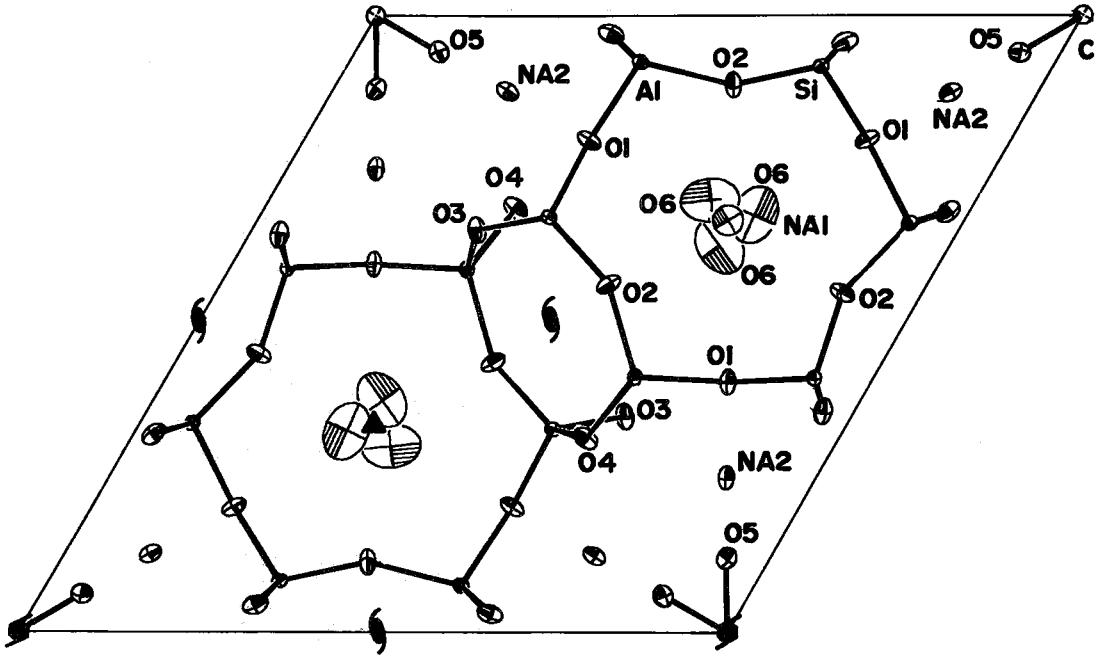

FIG. 3. Diagramatic projection of the trial structure down [001], showing the site nomenclature and also the symmetry elements for space group $P6_3$.

Obviously, the starting model is not adequate to reveal the details of the structure beyond those already seen by Jarchow (1965). In order to develop a more useful model, it is necessary to review the possible origins of the superstructures observed in the diffraction pattern of cancrinite specimens. The superstructures are similar, in that they are one-dimensional in nature and affect the *z*-axis repeat. The repeats, based on the superstructure, are consistent with integral numbers of substructure repeats and can increase the unit cell to as much as 16 times that of the substructure (Brown & Cesbron 1973). The intensity of the superstructure reflections seen on X-ray-diffraction photographs (Fig. 2) are, in general, much weaker than those of the substructure. However, on electron-diffraction photographs, owing to the more complex diffraction process, they are much more apparent (Fig. 5) and can approach the intensity of the substructure reflections.

Rationalization of the superstructure is based on two models, both of which are theoretically reasonable : 1) substitutional or positional ordering (or both) of interframework cations and anions (see Foit *et al.* 1973), and 2) periodic variation in the stacking sequence of the framework giving a sequence transitional between those of the cancrinite structure ABAB ... and the sodalite structure ABCABC ... (see Rinaldi & Wenk 1979). For the CO_3^{2-}-rich cancrinites, the first model appears to be the most appropriate, based on experimental observations. The high-temperature work of Foit *et al.* (1973) on CO_3^{2-}-rich material showed that on heating, the superstructure intensity decreased with time, whereas that of the substructure remained constant. On prolonged heating (Chen 1970), the position of the superstructure reflections changed as a function of time, indicating its potentially incommensurate nature. The above behavior is difficult to explain by changes in the stacking sequence, which involve the reorganization of the framework. Model 2 has been suggested for those cases where the intensity of the superstructure approaches that of the substructure (Merlino & Orlandi 1977a).

Afghanite is an example of a cancrinite of this type; it has been assigned a tentative stacking sequence of ABABACAC by Merlino & Mellini (1976). Although the electron-diffraction pattern (Rinaldi & Wenk 1979) shows a reasonably intense superstructure, however, the X-ray-diffraction pattern (Bariand *et al.* 1968) shows the extra reflections to be very much

weaker than those of the substructure. Rinaldi & Wenk (1979) observed lattice fringes with the TEM for both afghanite and franzinite and, following the proposals of Merlino & Mellini (1976) and Merlino & Orlandi (1977a, b), interpreted these in terms of differing stacking sequences. Cancrinites, which have been associated with model 2, are in general SO_4^{2-}-rich and CO_3^{2-}-poor. As yet there have been no successful structure refinements of the proposed polytypes; published *R*-indices vary from 16 to 30% (Rinaldi & Wenk 1979, Bariand *et al.* 1968, Barrer *et al.* 1970, Mazzi *et al.* 1981).

Foit *et al.* (1973) also noted that the superstructure reflections were still observable after the heating experiments, although greatly reduced in intensity. It is possible that such residual intensity could perhaps be assigned to a type-2 model. More recently, prolonged heating at 400°C of sacrofanite (Burragato *et al.* 1980) was shown to have no effect at all on the superstructure, which would suggest that, in this case, it was due in total to a type-2 origin. This material is SO_4^{2-}-rich with only minor CO_2 and H_2O and, therefore, differs from the CO_3^{2-}-rich cancrinites, which readily lose CO_2 and H_2O on heating. In order to determine the role of stacking variations in the cancrinite under study, it was decided that the structure should be imaged using high-resolution transmission electron microscopy (HRTEM) so that any periodic variation in the stacking sequence could be incorpororated into the structural model.

High-Resolution Transmission Electron Microscopy

In order to see the stacking sequence, a section containing the 6_3 axis is necessary; the most useful section is parallel to (010), *i.e.*, perpendicular to [210]. Figure 4 shows a schematic view of the framework down [210], illustrating a hypothetical example of a stacking variation ABACBA... that may be observed in this projection.

The microscope used was a JEM 100B operating at 100 kV with objective aperture centred about the incident beam of 50 μm (*i.e.*, radius of $\approx$ 0.42 Å^{-1}), a 150 μm condenser aperture and a 200 to 500K magnification factor. The specimen was prepared by ion-thinning a single-crystal section obtained from a polished thin section having the crystal oriented subparallel to (010). Twenty-nine substructure beams plus the included superstructure intensities were used to produce the bright-field image shown in Figure 5. The electron-diffraction pattern (Fig. 5) corresponding to the image was photographed both before and after imaging and was not observed to change. Note that this pattern shows 00*l*-type substructure re-

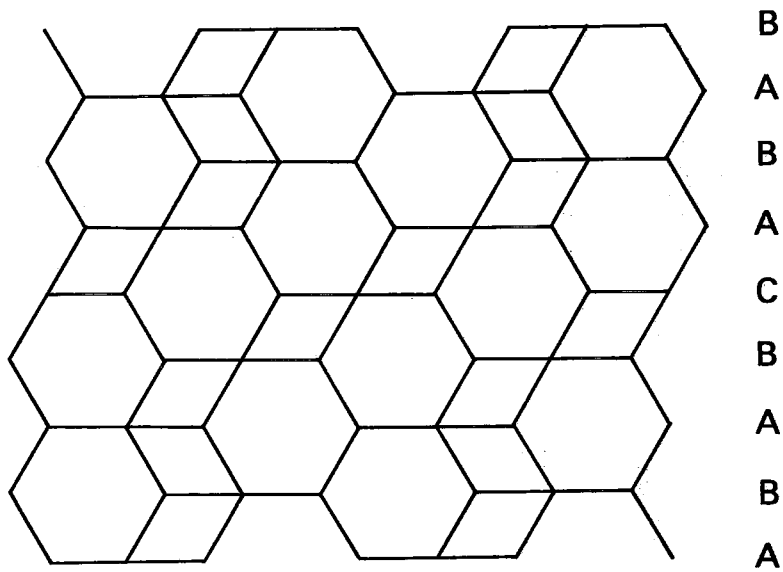

FIG. 4. Hypothetical diagram of the Al/Si framework projected down [210]. Shown is a *C*-type stacking fault in the regular ABAB... type of stacking sequence.

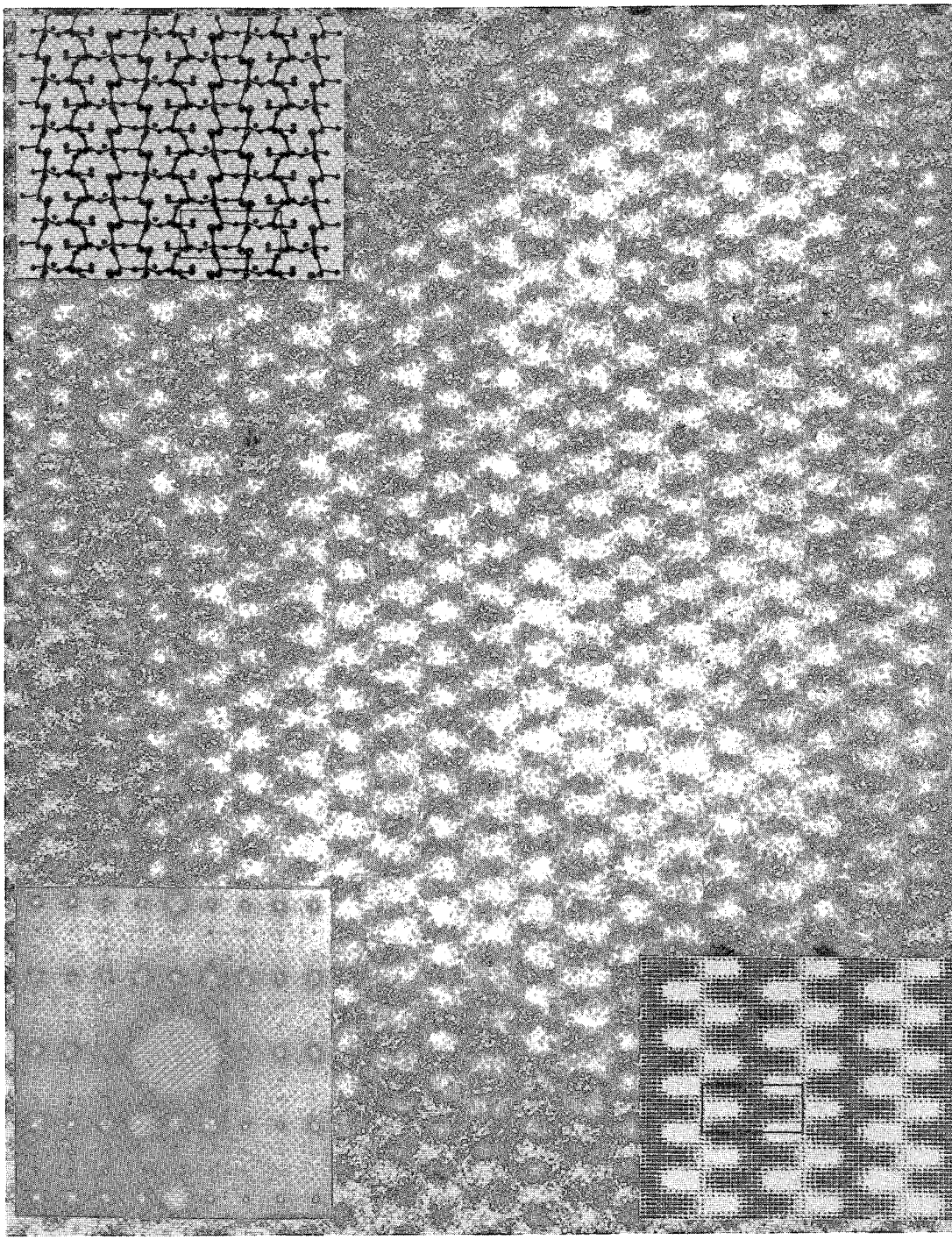

FIG. 5. High-resolution transmission electron micrograph down the [210]. Inset at lower left is the electron-diffraction pattern used in the imaging process. Inset at lower right is the scaled and oriented representation of the calculated image. Inset at top left is a projection of the trial structure down [210]. The rectangular boxes correspond to one substructure cell, the small edge of which is approximately 5 Å in magnitude.

flections when l is odd; these are forbidden in space group $P6_3$ and were not observed on the X-ray-diffraction photograph (Fig. 2). On tilting the specimen slightly, they changed intensity and, therefore, were interpreted as artifacts, mainly due to multiple diffraction, with perhaps a small part due to the superposition of a superstructure reflection.

Also inset in Figure 5 is a projection of the trial structure down [210], which is scaled and oriented so as to superimpose directly on a relevant part of the electron micrograph. The positioning was verified by comparing a calculated image with the one observed. Calculations were made using the multislice method (Goodman & Moodie 1974, Cowley & Moodie 1957) with a program developed by O'Keefe *et al.* (1978) and O'Keefe & Buseck (1979) for the calculation of images of minerals.

Owing to the extreme instability of the substance in the electron beam, it was not possible to experimentally obtain the usual through-focus series of images. Instead, calculations were made for a variety of foci in addition to thickness. Systematic trends emerged and it was possible to match the observed image shown in Figure 5 with a thickness of approximately 50 Å at an underfocus of –900 Å. In this image, areas of light contrast correspond to regions of low electrostatic potential. This calculated image is also shown correctly scaled and oriented as an inset in Figure 5.

Careful study of the image revealed that the stacking sequence was of the type ABAB . . ., with neither systematic deviations nor even random stacking faults. Therefore, in this case, a model-2 contribution to the superstructure intensity could be eliminated completely.

Refinement of the Structure

It has been experimentally established that the appearance of the superstructure in this substance is not due to alternate stacking sequences; furthermore, from the trial refinement, it was determined that the Al/Si frame-

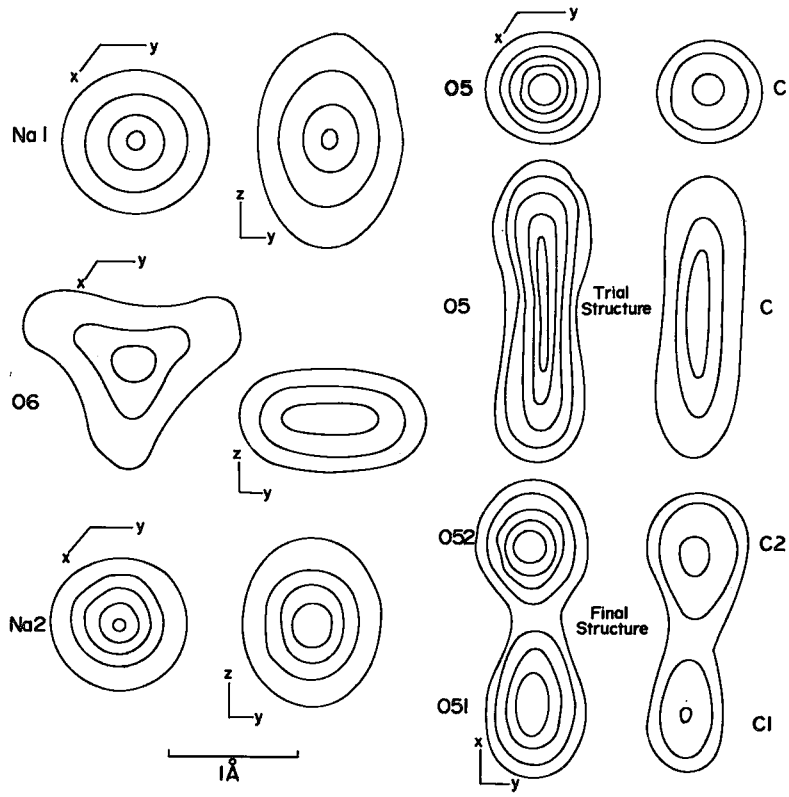

FIG. 6. Fourier sections of electron density through the interframework atom sites derived from the observed structure factors and calculated phases.

work was positionally well defined; the superstructure thus must originate from substitutional or positional ordering (or both) of the non-framework ions. Large-scale Fourier maps of electron density were prepared for the channel and cage volumes using the observed structure-factors and phase information from the trial refinement, in order to detect details that would lead to a better model of the structure.

The environment of the small cage was examined; the electron density on the anion site O6 (Fig. 6) was seen to be ellipsoidal in *yz* sections but triangular in *xy* sections. This triangular feature was also noted by Jarchow (1965); his procedure of moving the atom off the 3-fold axis and disordering it was followed. The cation position NA1 shows an electron density distributed as an ellipsoid of rotation about the 3-fold axis; it is elongate down this axis, but not sufficiently extensive to warrant positionally disordering the atom responsible for it in more than one position. Therefore, this atomic position was kept identical to that of the trial structure.

The large channel also was investigated; the cation position approximated an isotropic distribution of density, with no indication of systematic positional disorder. However, the anion group CO_3^{2-} showed extreme anisotropism in the distribution of density, with the direction of elongation parallel to the *z* axis. In the *xy* sections the individual atoms of the group showed reasonably circular cross-sections of density. In order to account for this distribution of density, the position was split into two nonequivalent positions 1.6 Å apart down the *z* axis. Refinement was continued using the modified set of atom positions and, on the final cycle, after varying all refinable parameters, the structure converged with a conventional *R* factor of 2.8%.

Fourier maps were again prepared using the F_o values and the new phases. The maps now showed two well-separated maxima for the CO_3^{2-} groups (Fig. 6), in accord with the postulated positions, and three maxima for the O6 position. All other atom positions were examined for positional disorder, but none was found, and the average structure was considered to the fully refined at this point. Table 2 lists the observed and calculated structure factors together with their phase angles; this table is available at nominal charge from Depository of Unpublished Data, CISTI, National Research Council of Canada, Ottawa, Ontario K1A 0S2. Final positional parameters are shown in Table 3, and the anisotropic temperature factors are presented in Table 4.

TABLE 3. OCCUPANCIES, POSITIONAL AND ISOTROPIC THERMAL PARAMETERS

atom	equi-point position	site content	x	y	z	$B_{(equiv)}$ Å^2	
Framework atoms							
O1	c	O	.2027(2)	.4043(2)	.6574(5)	1.16	
O2	c	O	.1131(2)	.5635(2)	.7281(7)	1.59	
O3	c	O	.0295(2)	.3487(2)	.0610(5)	1.14	
O4	c	O	.3131(2)	.3566(2)	.0439(5)	1.25	
T1	c	Si	.3277(1)	.4125(1)	3/4	.54	
T2	c	Al	.0752(1)	.4125(1)	.7510(3)	.60	
Non-framework atoms†							
O51	c	.38 O+.62 []	.0572(8)	.1163(8)	.6729(25)	2.8	ch†
O52	c	.38 O+.62 []	.0587(8)	.1194(8)	.9134(30)	3.4	ch
O6	c	.33 O	.6246(12)	.3243(42)	.6875(25)	6.3	cg
C1	a	.38 C+.62 []	0	0	.6729(25)	2.7	ch
C2	a	.38 C+.62 []	0	0	.9134(30)	4.3	ch
NA1	b	1.00 Na	2/3	1/3	.1339(11)	3.9	cg
NA2	c	.67 Na+.25 Ca +.08 []	.1232(1)	.2490(1)	.2959(3)	1.5	ch

† chemical symbol [] is vacancy.
ch located in channel.
cg located in cage.

TABLE 4. ANISOTROPIC† TEMPERATURE PARAMETERS × 10^4

atom	U_{11}	U_{22}	U_{33}	U_{12}	U_{13}	U_{23}
Framework atoms						
O1	113(9)	218(10)	110(8)	113(8)	5(8)	17(9)
O2	221(10)	115(8)	268(13)	113(8)	14(12)	12(11)
O3	115(9)	220(10)	99(11)	91(8)	35(8)	45(9)
O4	159(10)	225(11)	91(10)	133(9)	13(8)	45(9)
T1	65(3)	78(3)	65(3)	39(2)	2(4)	3(4)
T2	72(3)	86(3)	70(3)	43(3)	0(4)	6(4)
Non-framework atoms						
O51	124(34)	127(33)	801(86)	55(29)	0(38)	42(39)
O52	147(40)	144(38)	1004(98)	86(34)	5(49)	-83(49)
O6	982(115)	1073(156)	332(60)	714(201)	-49(56)	-53(104)
C1	207(60)	207(60)	619(161)	103(31)	0	0
C2	112(52)	112(52)	1411(348)	56(26)	0	0
NA1	312(10)	312(10)	849(34)	156(5)	0	0
NA2	114(4)	179(5)	271(8)	94(4)	-18(5)	-12(5)

† where temperature factor = $\exp\left[-2\pi^2 \sum_{i=1}^{3} \sum_{j=1}^{3} (U_{ij} a_i^* a_j^* h_i h_j)\right]$

Description of the Structure

The general features of the structure have been described in the introductory paragraphs; only further details will be presented here. Important interatomic distances are shown in Table 5, and interframework angles in Table 6. The average tetrahedral bond-lengths (Table 5), 1.612 and 1.733 Å, can be assigned to Si–O and Al-O respectively. A calculation following Baur (1978) shows that the 1.612 Å distance corresponds to full occupancy by Si. Therefore, as the ratio of Al:Si is 1:1, by implication the 1.733 Å distance corresponds to full occupancy by Al. The framework is therefore fully ordered. Bond-valence calculations (Brown & Shannon 1973) show that the bond-valence deficiency on the framework oxygen atoms is predominantly satisfied by the cations on the NA2 position,

TABLE 5. SELECTED INTERATOMIC DISTANCES† AND BOND STRENGTH (VALENCE UNITS)††

bond	Å	Bond strength (vu)	bond	Å	Bond strength (vu)
T1-01	1.608(3)	1.038(8)	T2-01	1.728(3)	.762(5)
-02	1.601(4)	1.057(11)	-02	1.717(3)	.783(5)
-03	1.619(5)	1.008(3	-03	1.741(3)	.738(5)
-04	1.621(3)	1.003(7)	-04	1.747(3)	.727(5)
Mean	1.612(3)	Total 4.106	Mean	1.733	Total 3.011
*Calculated (Si) 1.616		Expected** 4			Expected 3
Na1-01 × 3	2.863(3)	0.261(10)	C1-051 × 3	1.268(9)	
-02 × 3	2.450(5)	0.510(10)			
-06[a]	2.335(23)	0.208(5)	C2-052 × 3	1.302(9)	
-06[b]	2.874(15)	0.086(1)			
Mean for [8]	2.644	Total 1.065			
[4]	2.421	Expected 1			
	trigonal bipyramid			octahedral	
Na2-01	2.507(3)	0.154(0)	Na2-01	2.507(3)	.154(0)
-03	2.427(4)	0.177(1)	-03	2.427(4)	.177(1)
-04	2.444(3)	0.172(0)	-04	2.444(3)	.172(0)
-051[a]	2.440(11)	0.173(3)	-052[a]	2.414(14)	.182(4)
-051[a]	2.431(21)	0.176(6)	-052[b]	2.424(21)	.178(6)
-051[b]	2.412(12)	0.183(3)	-052[b]	2.432(12)	.176(3)
Mean	2.444		Mean	2.441	
-03	2.859(3)	0.088(0)	-03	2.859(3)	.088(0)
-04	2.891(6)	0.084(0)	-04	2.891(6)	.084(0)
Mean	2.552	Total 1.208	Mean	2.550	Total 1.212
		Expected 1.17			Expected 1.17

† a = above : b = below
* according to Baur (1978) for site filled with Si
†† universal curves
** expected from site population (see Table 2)

TABLE 6. SELECTED FRAMEWORK ANGLES

	tetrahedral		
01-T1-02	108.2(2)	01-T2-02	107.2(1)
-03	107.1(1)	-03	109.1(2)
-04	110.5(1)	-04	106.0(2)
02-T1-03	112.4(2)	02-T2-03	114.7(2)
-04	112.2(2)	-04	114.6(2)
03-T1-04	106.5(2)	03-T2-04	104.8(1)
Mean	109.5	Mean	109.4
	bridging		
T1-01-T2	142.3(2)		
T1-02-T2	152.8(2)		
T1-03-T2	132.8(2)		
T1-04-T2	132.9(2)		
Mean	142.2		

which lie within the channel, with the exception of the oxygen on the O2 position, which is too remote and satisfied solely by the cage cation. The calculation shows the bond-valence deficiency on O2 to be 0.17 valency units (v.u.). The NA1 position is closely co-ordinated to three O2 oxygen atoms and the oxygen at O6, which is part of a hydrogen-bonded water molecule. These hydrogen bonds are weak and, according to Brown (1976), have a valency of less than 0.1 v.u. As the O6 . . . .O distance must be greater than 3 Å, this valency must be dispersed over five framework oxygen (3 x O2, O1 and O3) that are within hydrogen-bonding distance. The directionality of the hydrogen bonds formed is the probable cause of the relatively well-resolved positional disorder of the O6 oxygen atom.

Both the population refinement and the bond-valence sum show the NA1 site to be fully occupied by Na^+. It is unlikely that this structural position will ever be systematically defective, owing to O2 charge requirements, unless there is a corresponding increase in the Si/Al ratio of the framework. Furthermore, owing to the unresolved positional disorder of the NA1 and O6 sites parallel to the z axis, the cage cations and anions will not contribute to the one-dimensional superstructure of this cancrinite.

The configuration of the interchannel cation NA2 and anion groups positionally conforms to space group $P6_3$ symmetry. However, as there is only one cation position, the refinement must show this site to be completely disordered with respect to Na, Ca and vacancies.

Both the site-population refinement (Table 3) and bond-valence sums (Table 5) confirm the chemistry (Table 1) of the NA2 site. The CO_3^{2-} groups lie on two nonequivalent 2-fold positions; the population refinement shows these to be equally occupied by 0.4 of a CO_3^{2-} group. Because of the close proximity of the positions, only one can be occupied at any one time and, therefore, the maximum possible occupancy for total disorder would be 0.5 groups per site. Bond-valence calculations (Table 5) about the

cation site NA2 show that the two possible co-ordinations of NA2 (depending on which CO_3^{2-} position is occupied; see Fig. 7) are electrostatically equivalent. However, the refinement does show a slightly larger temperature-factor for the CO_3^{2-} group associated with octahedral co-ordination, which could, in turn, be interpreted as a slightly higher occupancy due to a correlation that exists between these two parameters. However, as both Na and Ca are usually irregularly co-ordinated, a preference is not expected in this case. The substantial temperature-factor component parallel to the z axis for the CO_3^{2-} is probably due, in part, to a more subtle positional disorder, depending on the type of cation (Na or Ca) or vacancy that it is co-ordinating. However, there is no marked anisotropy of the NA2 site, indicating that the framework tends to be insensitive to the type of cation or vacancy on this site. Chemical variation on the NA2 site is accommodated solely by the positioning of the anion groups within the channel.

Origin of the Superstructure

According to the space-group symmetry, the chemical formula shows that there is a deficiency in each NA2 cation site of 0.08 ions and a deficiency of double that in the CO_3^{2-} group. Therefore, the substitutions that must be considered are Na $\rightleftarrows$ Ca$\rightleftarrows$ vacancy for the NA2 position and $CO_3^{-}\rightleftarrows$ vacancy for the channel-anion positions. Superstructures might easily arise from ordering of such vacancies. As previously discussed, it seems unlikely that the cage environment contributes significantly to the superstructure. However, owing to the variety of orientations possible for the water molecule, it is conceivable that these can indirectly stabilize certain vacancies in the large channel by providing extra charge to the O1 framework

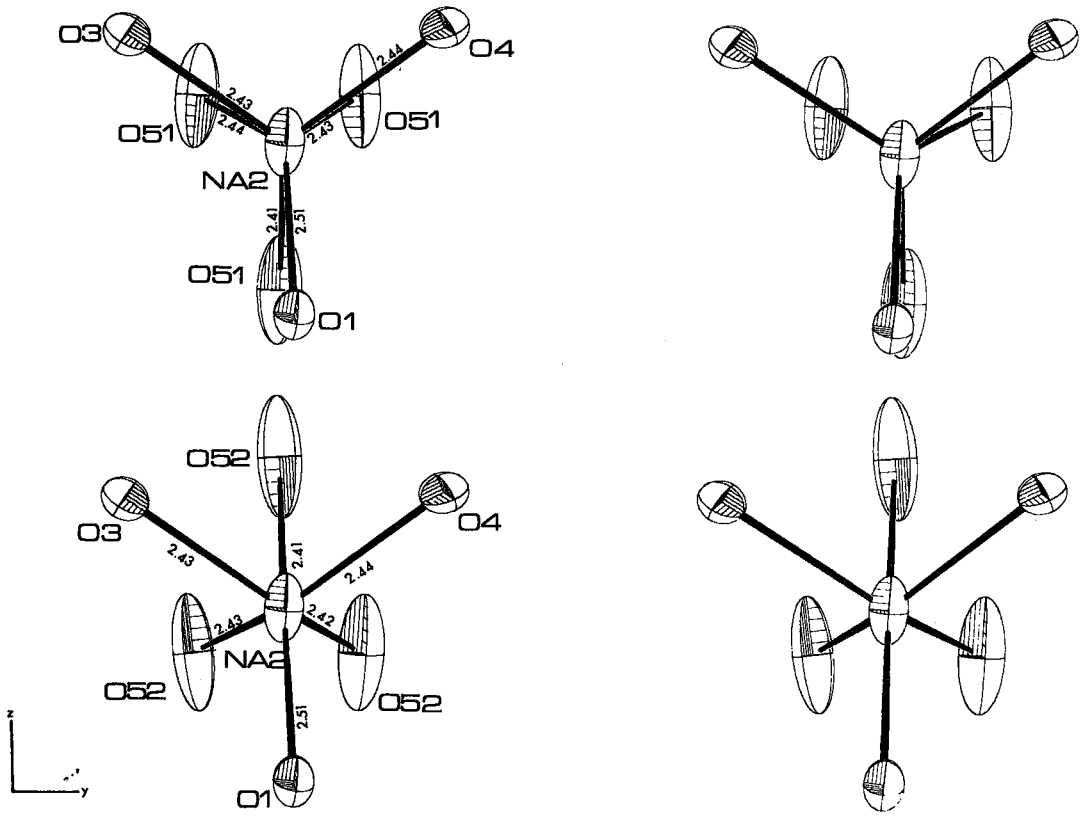

FIG. 7. Stereographic drawing in the vicinity of the NA2 cation site showing the position of framework and CO_3^{2-}-group oxygen atoms co-ordinating this site for the two arrangements of the CO_3^{2-} groups.

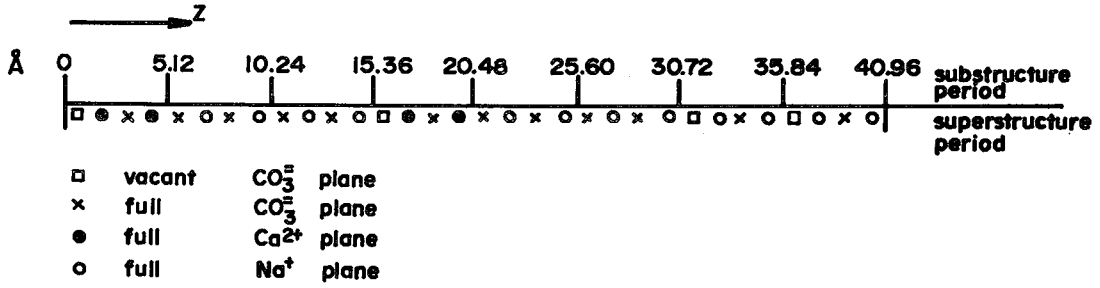

FIG. 8. Ordering pattern used for the generation of the calculated superstructure, the intensities of which are compared with those observed in Table 7.

oxygen when required through hydrogen bonding. By far the most important contribution to the superstructure is from the arrangement of the interchannel cations, anions and vacancies.

The period of the superstructure along z is 40.94 Å; from the results of the chemical analysis (Table 1), the channel contains approximately 32 Na^+, 12 Ca^{2+} and 13 CO_3^{2-} per supercell. The stoichiometric composition should be 48 ($Na^+ + Ca^{2+}$) and 16 CO_3^{2-} groups (32 positions half-occupied). Therefore, the nature of the superstructure is controlled by 3 to 4 CO_3^{2-}-group omissions with subsequent rearrangement of cations and vacancies on the NA2 position.

In order to generate a likely pattern from the great number of possibilities, assumptions were made so that the problem could be converted to a one-dimensional calculation. This would make a computer simulation of all the superstructure intensity-patterns feasible. If we choose to match only 00*l*-type reflections, we are concerned only with an arrangement of points of differing weight of electron density along the z axis, these are in known positions. In order to simplify the problem still further we can consider only four types of points corresponding to 3Ca, 3Na, $3CO_3$ or 3 vacancies, for neutral atoms points of weight 60, 33, 30, 0, respectively. Using the superperiodic spacing (40.94 Å), the known positions of the points, and X-ray and electron scattering factors for neutral atoms (Doyle & Turner 1968), we can calculate the intensities of the 00*l* reflections using the standard structure-factor equations. After correcting for Lorentz and polarization effects, these calculated intensities can be compared directly with the observed patterns of intensity.

As we know the number of points involved and with the assumption that they are only of the types described above, a computer program was written to generate all possible combinations. The best match in pattern is shown diagrammatically in Figure 8 and the corresponding match in intensity in Table 7. The comparison is done only on a semiquantative basis; a closer fit could perhaps be attained by allowing weights to vary and then optimizing the difference between observed and calculated intensities, perhaps by the least-squares method. However, owing to the difficulty of measuring enough of these weak superstructure-reflections to obtain good statistical integrity, it was not

TABLE 7. OBSERVED AND CALCULATED SUPERSTRUCTURE INTENSITIES (00ℓ)†

	X-ray diffraction		Electron diffraction††	
	observed	calculated	observed	calculated
ℓ				
1				
2			hidden by incident beam scatter	
3	hidden			
4	by			
5	incident		100	100
6	beam		20	20
7	scatter			1
8		SUBSTRUCTURE (EXTINCT)	present	4
9				3
10			5	6
11			15	9
12				0
13	100	100	20	17
14	50	65	5	8
15		19		2
16		SUBSTRUCTURE		
17	hidden			2
18	by white		5	4
19	radiation		5	3
20	streak			0
21			5	2
22		6	5	1
23		0		0
24		SUBSTRUCTURE (EXTINCT)		2
25		0		0
26		4	1	0
27	10	14	1	0
28		0		0
29	20	28	5	2
30		18		0
31		6		0
32		SUBSTRUCTURE		

† ℓ index base on super-period of 40.94 Å.
†† visually estimated from photographs taken for varying lengths of exposure only semi-quantitative. Blanks in table correspond to unobserved intensity values. Dynamical aspects of electron diffraction not considered.

possible to do this with this substance. Even so, the fit is sufficiently good to show that a representative superstructure can be generated solely from the ordering of interchannel ions.

Conclusions

We conclude from this work that a useful model has been developed to investigate cancrinite-type structures and, by association, certain aspects of the structure of the sodalite group of minerals. The absence of stacking sequences different from the type ABAB . . . has been experimentally established and, therefore, in this case, precludes their role in the generation of the observed superstructure. The positions and intensities of the superstructure reflections can be adequately relationalized by substitutional disorder on atom sites that are positionally defined by the $P6_3$ symmetry. A possible arrangement for Na^+, Ca^{2+}, CO_3^{2-} and vacancy over the available sites according to the results of the chemical analysis has been established through computer simulation of the 00*l* superstructure intensities and semiquantitative comparison with the observed pattern. However, a more rigorous approach using modulation theory may be more fruitful for explaining the superstructures of more complex cancrinite-type materials.

Acknowledgements

Financial assistance was rendered by an NSERC operating grant to H. D. Grundy and by an NSF grant (EAR 79–26375) to P. R. Buseck. Electron microscopy was performed in the Arizona State University Facility for High Resolution Electron Microscopy, established with support from the NSF Regional Instrumentation Facilities Program, grant CHE 79–16098. In particular, we thank Dr. P. R. Buseck for his support and encouragement and also Dr. I. McKinnon and Mr. M. J. Wheatley for their patience and instruction in the use of the electron microscopes.

References

Bariand, P., Cesbron, F. & Giraud, R. (1968): Une nouvelle espèce minérale: l'afghanite de Sar-e-Sang, Badakhshan, Afghanistan. Comparaison avec les minéraux du groupe de la cancrinite. *Soc. franç. Minéral. Crist. Bull.* **91**, 34-42.

Barrer, R.M., Cole, J.F. & Villiger, H. (1970): Chemistry of soil minerals. VII. Synthesis, properties and crystal structures of salt-filled cancrinites. *J. Chem. Soc.* **9A**, 1523-1531.

Baur, W.H. (1978): Variation of mean Si–O bond lengths in silicon–oxygen tetrahedra. *Acta Cryst.* **B34**, 1751-1756.

Brown, I.D. (1976): On the geometry of O–H . . . O hydrogen bonds. *Acta Cryst.* **A32**, 24-31.

——— & Shannon, R.D. (1973): Empirical bond-strength – bond-length curves for oxides. *Acta Cryst.* **A29**, 266-282.

Brown, W.L. & Cesbron, F. (1973): Sur les surstructures des cancrinites. *C.R. Acad. Sci. Paris* **276**(D), 1-4.

Burragato, F., Parodi, G. C. & Zanazzi, P.F. (1980): Sacrofanite – a new mineral of the cancrinite group. *Neues Jahrb. Mineral. Abh.* **140**, 102-110.

Chen, S.M. (1970): *A Chemical, Thermogravimetric and X-Ray Study of Cancrinite.* M.Sc. thesis, McMaster Univ., Hamilton, Ont.

Cowley, J.M. & Moodie, A.F. (1957): The scattering of electrons by atoms and crystals. I. A new theoretical approach. *Acta Cryst.* **10**, 609-619.

Doyle, P.A. & Turner, P.S. (1968): Relativistic Hartree-Fock X-ray and electron scattering factors. *Acta Cryst.* **A24**, 390-397.

Foit, F.F., Jr., Peacor, D.R. & Heinrich, E.W. (1973): Cancrinite with a new superstructure from Bancroft, Ontario. *Can. Mineral.* **11**, 940-951.

Goodman, P. & Moodie, A. F. (1974): Numerical evaluation of *N*-beam wave functions in electron scattering by the multi-slice method. *Acta Cryst.* **A30**, 280-290.

Jarchow, O. (1965): Atomanordnung und Strukturverfeinerung von Cancrinit. *Z. Krist.* **122**, 407-422.

Mazzi, F. & Tadini, C. (1981): Giuseppettite, a new mineral from Sacrofano (Italy), related to the cancrinite group. *Neues Jahrb. Mineral. Monatsh.*, 103-110.

Merlino, S. & Mellini, M. (1976): Crystal structures of cancrinite-like minerals. *In* Zeolite 1976, Proc. International Conference on the Occurrence, Properties, and Utilization of Natural Zeolites (Tuscon). Program Abstr., 47.

——— & Orlandi, P. (1977a): Liottite, a new mineral in the cancrinite–davyne group. *Amer. Mineral.* **62**, 321-326.

——— & ——— (1977b): Franzinite, a new mineral phase from Pitigliano (Italy). *Neues Jahrb. Mineral. Monatsh.*, 163-167.

NITHOLLON, P. & VERNOTTE, M.P. (1955): Structure cristalline de la cancrinite. *Publ. Sci. Tech. Ministère Air (France), Notes Tech.* **53**, 1-48.

O'KEFFE, M.A. & BUSECK, P.R. (1979): Computation of high resolution TEM images of minerals. *Amer. Cryst. Assoc. Trans.* **15**, 27-46.

———, ——— & IIJIMA, S. (1978): Computed crystal structure images for high resolution electron microscopy. *Nature* **274**, 322-324.

PAULING, L. (1930): The structure of some sodium and calcium aluminosilicates. *Nat. Acad. Sci. Proc.* **16**, 453-459.

RINALDI, R. & WENK, H.-R. (1979): Stacking variations in cancrinite minerals. *Acta Cryst.* **A35**, 825-828.

SCHULZ, H. (1970): Struktur- und Uberstrukturuntersuchungen an Nosean–Einkristallen. *Z. Krist.* **131**, 114-138.

STEWART, J.M., MACHIN, P.A., DICKINSON, C.W., AMMON, H.L., HECK, H. & FLACK, H. (1976): The X-RAY system of crystallographic programs. *Univ. Maryland Comp. Ctr. Tech. Rep. TR–446.*

VAN PETEGHEM, J. & BURLEY, B.J. (1962): Studies on the sodalite group of minerals. *Roy. Soc. Can. Trans.* **56**, *Ser. III, Sect. III*, 37-53.

Received October 1981, revised manuscript accepted March 1982.